Paleoseismology of the Tijeras fault near Golden, New Mexico

Keith I. Kelson, Christopher S. Hitchcock, and J. Bruce J. Harrison

1999, pp. 201-209. https://doi.org/10.56577/FFC-50.201

in:

Albuquerque Geology, Pazzaglia, F. J.; Lucas, S. G.; [eds.], New Mexico Geological Society 50 th Annual Fall Field Conference Guidebook, 448 p. https://doi.org/10.56577/FFC-50

This page is intentionally left blank to maintain order of facing pages.

PALEOSEISMOLOGY OF THE TIJERAS FAULT NEAR GOLDEN, NEW MEXICO

KEITH I. KELSON[1], CHRISTOPHER S. HITCHCOCK[1], and J. BRUCE J. HARRISON[2]
[1]William Lettis & Associates, Inc., 1777 Botelho Drive, Suite 262, Walnut Creek, CA 94596; kelson@lettis.com; hitch@lettis.com;
[2]Earth and Environmental Sciences Department, New Mexico Tech, Socorro, NM 87801; bruce@nmt.edu

Abstract—The 100-km-long Tijeras-Cañoncito fault system is a potential seismogenic source that extends between the Santa Fe and Albuquerque metropolitan areas of New Mexico. The fault system accommodates east–west crustal extension and provides structural linkage between the Española and Albuquerque basins of the active Rio Grande rift. At the Adobe Camp site northeast of Albuquerque, we conducted detailed trenching to assess the near-surface location, timing, and style of late Quaternary deformation on the southern Tijeras fault, a major component of the Tijeras-Cañoncito fault system. At Adobe Camp, the fault consists of two main strands that may represent a positive half-flower structure. The eastern fault strand is vertical and coincides with a left-deflection in a west-flowing arroyo. The western fault strand has reverse fault geometry and dips moderately eastward; it likely merges with the eastern vertical strand in the shallow subsurface (about 30 to 40 m depth). The western strand has placed bedrock over late Quaternary deposits and coincides with northwest-facing scarps that truncate piedmont surfaces. Field relations suggest that vertical separation was produced along the western fault strand, whereas lateral offset occurred primarily on the eastern fault strand. Trench and arroyo-wall exposures show that two colluvial deposits were shed from the fault scarps along the western fault strand. The lower colluvial deposit is faulted, whereas the upper colluvium is not, thereby indicating two faulting events. The ages of these earthquakes are poorly constrained because of uncertainties in the ages of the faulted and unfaulted colluvia. However, based on the relative degree of soil development and stratigraphic position, we estimate that the colluvia most likely are late Pleistocene (11–130 ka). Our interpretation is that the scarp-derived colluvia were deposited following two surface-rupturing earthquakes along the southern Tijeras fault during the late Pleistocene. If these earthquakes ruptured the entire 41-km-long southern part of the Tijeras fault, they may have been as large as moment magnitude (M_W) 7.0.

INTRODUCTION

The Rio Grande rift in northern and central New Mexico contains numerous poorly characterized, potentially active faults, many of which exhibit evidence of late Pleistocene or Holocene movement (Machette, 1978; Machette and McGimsey, 1982; Machette and Personius, 1984; Abbott and Goodwin, 1995; Wong et al., 1995, 1996; Kelson et al., 1996; Machette et al., 1998). Many of these faults may pose a seismic hazard to the populated Albuquerque-Santa Fe metropolitan region. The Tijeras-Cañoncito fault system extends approximately 100 km from Albuquerque nearly to Santa Fe, and consists of several northeast-striking, nearly vertical faults, including the Tijeras, Guiterrez, Zuzax, San Lazarus, Los Angeles, and Lamy faults (Lisenbee et al., 1979; Abbott and Goodwin, 1995). Previous workers have shown that the Tijeras-Cañoncito fault system exhibits evidence of recurrent activity during the late Cenozoic (<25 Ma), including Quaternary displacement at three localities along the Tijeras fault (Lisenbee et al., 1979; Abbott and Goodwin, 1995; GRAM/William Lettis & Associates, 1995). The fault system crosses the epicentral area of the 1918 Cerrillos earthquake, the largest historical earthquake located within the northern Rio Grande rift (M_L 4.5–5.5; Olsen, 1979). Wong et al. (1995) estimated that the fault system could generate earthquakes between moment magnitude (M_W) 6.6 and 7.0. Thus, obtaining better paleoseismic (ancient earthquake) information on the Tijeras-Cañoncito fault system is critical for realistically assessing seismic hazard in the region.

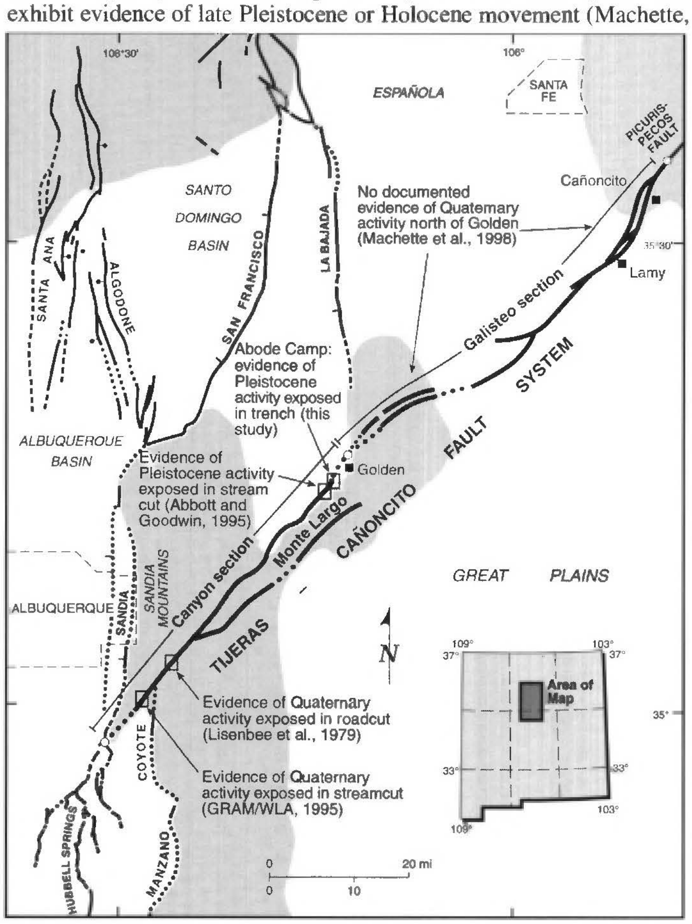

FIGURE 1. Regional fault map showing known localities of Quaternary activity along the Tijeras-Cañoncito fault system, and fault sections chosen by Machette et al. (1998).

Our research provides initial paleoseismic information on the timing and style of late Quaternary faulting along the southern part of the Tijeras fault, a major component of the Tijeras-Cañoncito fault system (Fig. 1). We analyzed aerial photography, completed an aerial overflight of the fault, and conducted field reconnaissance of potential paleoseismologic sites along the fault between Tijeras Canyon and Golden, New Mexico. Based on this information, we selected a site near Golden in order to obtain data on the late Quaternary earthquake history (paleoseismology) of the southern Tijeras fault. In October and November 1997, we excavated three trenches across strands of the fault, and mapped a fault exposure within an arroyo bank. This paper summarizes the results of our research, which was conducted for the U.S. Geological Survey's National Earthquake Hazard Reduction Program (Kelson et al., 1998).

GEOLOGIC SETTING

The Tijeras-Cañoncito fault system separates the southeastern Española basin portion of the Rio Grande rift from the Great Plains physiographic province to the east, and extends through the Sandia Mountains to at least the eastern margin of the Albuquerque basin (Fig.

1). The fault system has had multiple episodes of movement (Lisenbee et al., 1979), and Neogene movement appears to have been in a left-lateral sense (Abbott and Goodwin, 1995). Because the fault cuts through the 3300-m-high Sandia Mountains and is not characterized by distinct normal displacement as with typical rift-margin faults, it is not necessarily easy to identify the Tijeras-Cañoncito fault system as a possible eastern margin of the active Rio Grande rift. However, the northeast strike of the fault system and left-lateral slip are consistent with interpretations of contemporary focal mechanisms that suggest a WNW–ESE orientation of the minimum principal stress near Albuquerque (Sanford et al., 1991). Evidence of Pleistocene movement (Lisenbee et al., 1979; Abbott and Goodwin, 1995; Kelson et al., 1998) supports the interpretation that the fault continues to accommodate rift extension and plays a role in rift extension between the en echelon Española and Albuquerque basins.

Very few data on the late Quaternary behavior of the Tijeras-Cañoncito fault system exist, although studies have addressed the pre-Quaternary deformational history of the fault system (Lisenbee et al., 1979; Abbott et al., 1995; Abbott and Goodwin, 1995). Lisenbee et al. (1979) noted displaced Quaternary colluvium in Tijeras Canyon directly east of Albuquerque, and Abbott and Goodwin (1995) described faulted fluvial deposits in a stream-cut exposure near Golden (Fig. 1). Smith et al. (1982) identified several fluvial terraces and geomorphic surfaces in Tijeras Canyon, and interpreted a complex geomorphic history for the canyon that may be related, in part, to movement along the fault. Recent research for Sandia National Laboratories (Kelson et al., 1994; SNL, 1995; GRAM/William Lettis & Associates, 1995) identified features possibly related to late Quaternary movement along the fault southwest of Tijeras Canyon. Their mapping identified displaced Pleistocene alluvium along the southernmost section of the fault, and delineated a complex intersection between the Tijeras fault and the Hubbell Springs fault on Kirtland Air Force Base. Lastly, Karlstrom et al. (1994) and Ferguson et al. (1996) have made geologic maps of the southern part of the Tijeras fault and geologic units in the Tijeras and Sandia Park quadrangles.

Because of the paucity of paleoseismic data, there are considerable uncertainties as to the location, length, and activity of potential fault-ruptures on the Tijeras-Cañoncito fault system. Lisenbee et al. (1979) identified several "structural segments" of the fault system on the basis of fault trace complexity and other structural relations. However, because of a lack of information on the timing of paleoearthquakes on all sections of the fault, Wong et al. (1995) defined potential rupture scenarios along four possible "rupture segments." More recently, Machette et al. (1998) described the Tijeras-Cañoncito fault system as having two primary physical sections: (1) the 41-km-long "Canyon" fault section between Albuquerque and Golden, and (2) the 51-km-long "Galisteo" section between Golden and the village of Cañoncito (Fig. 1). The purpose of this investigation is to provide information on the paleoseismic behavior of the southern (Canyon) section of the Tijeras fault.

SITE CHARACTERISTICS OF ADOBE CAMP

Geology and geomorphology

The Adobe Camp site is about 6 km southwest of Golden, New Mexico and about 1 km northeast of the fault exposure documented by Abbott and Goodwin (1995) (Fig. 1). The site includes a series of northwest-facing topographic scarps along previously mapped strands of the fault, as well as an arroyo exposure of deformed alluvial sediments in fault contact with highly fractured Oligocene(?) porphyritic rocks. The site lies along the western flank of Monte Largo, a 350-m-high horst block composed of Precambrian and Pennsylvanian bedrock bounded by the Tijeras fault on the west and the Guiterrez fault on the east (Kelley and Northrop, 1975). Near Adobe Camp, drainage derived from Monte Largo flows northwest primarily on Precambrian gneiss, schist and quartzite, across the Tijeras fault, into the broad Hagan basin, and ultimately to the Rio Grande via Arroyo Tonque.

The Adobe Camp site is characterized by hilly topography with west-flowing arroyos incised as much as 20 m into Quaternary pediment surfaces and underlying bedrock. The geomorphologic setting of the site is influenced by a 100-m-high quartzite hill directly southeast of the site. Multiple surfaces at the site are preserved primarily because the quartzite hill has protected the site from burial or erosion by the larger drainages to the northeast and southwest. Deposits at the Adobe Camp site thus were derived from drainages developed on primarily quartzite. Northwest-flowing drainages from the Monte Largo block have produced broad, high-level piedmont surfaces both to the northeast and southwest of the site.

The late Quaternary surficial deposits near Adobe Camp (Fig. 2) were mapped on the basis of stratigraphic, geomorphic, and pedologic criteria, including: (1) topographic position in a sequence of inset deposits or surfaces; (2) relative degree of surface modification (e.g., erosional dissection and surface smoothing); (3) relative degree of soil-profile development or other surface-weathering phenomena; (4) physical continuity and lateral correlation with other stratigraphic units; and (5) differences in clast lithologies. Surficial deposits and soils were characterized through field description of four 2-m-deep soil pits excavated on relatively flat, uneroded surface remnants.

The Adobe Camp site has remnants of three piedmont surfaces,

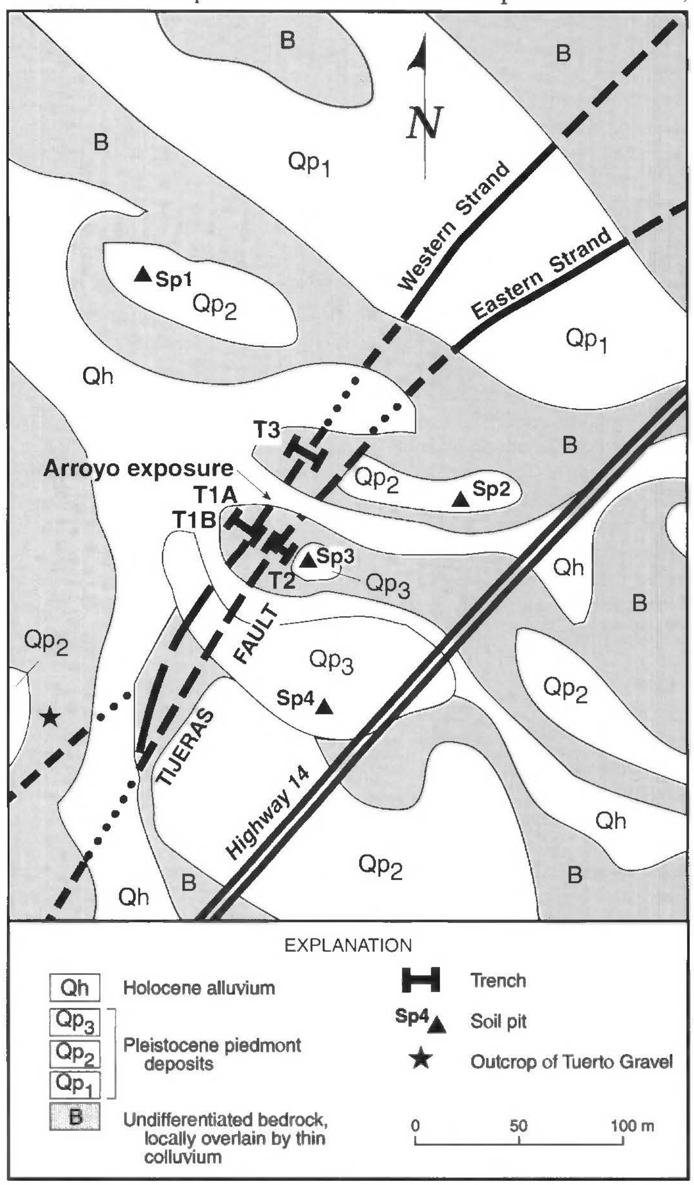

FIGURE 2. Surficial geologic map of the Adobe Camp study area, showing major strands of the Tijeras fault and locations of exploratory trenches and test pits.

which are mapped (from oldest to youngest) as units Qp1, Qp2, and Qp3 (Fig. 2). In general, units Qp1, Qp2, and Qp3 are thin (<3 m thick) gravel deposits unconformably overlying an erosional bedrock surface. Remnants of surface Qp1 are as much as 20-m above the active arroyo floors, and generally are broad smooth surfaces that slope gently to the northwest (Fig. 2). Clasts within the Qp1 deposits are mainly limestone, with minor quartzite, sandstone, felsite, and shale and were derived from large (unnamed) drainages that cross the Tijeras fault northeast and southwest of the Adobe Camp site. The clast lithologies reflect bedrock types exposed in the Monte Largo horst block and within the Tijeras fault zone (Kelley and Northrop, 1975; Abbott and Goodwin, 1995; Ferguson et al., 1996). Surface Qp2 is inset into the Qp1 piedmont surface, and is about 6 m lower in elevation. Gravel deposits associated with this surface contain predominantly quartzite clasts, with lesser amounts of sandstone, shale, felsite and limestone. The deposits were derived from small drainages developed on the quartzite hill southeast of the site and from local reworking of Qp1 materials (Fig. 2). Surface Qp3 is inset into the Qp2 surface, and is about 1 to 3 m lower in elevation than Qp2. Surface Qp3 remnants have been identified only within or directly adjacent to the Tijeras fault zone. Gravel deposits associated with the Qp3 surface consist of predominantly light-colored porphyritic rock (herein called "felsite"), with lesser amounts of quartzite. These deposits probably were derived from the Qp2 deposits and from felsite locally exposed along the Tijeras fault (Abbott and Goodwin, 1995).

In addition, the valley floors and active arroyos at Adobe Camp are underlain by Holocene alluvium (unit Qh, Fig. 2), and most slopes are mantled with thin, locally derived colluvium. Holocene alluvium consists of gravelly sand containing clasts of felsite, quartzite, sandstone, shale, and limestone. These deposits appear to be derived locally from deposits as well as bedrock outcrops. Based on the arroyo exposures, the Holocene alluvium is more than 3 m thick.

The Tijeras fault at Adobe Camp is a complex zone containing multiple fault strands, several of which may have had late Quaternary movement. At the site, the fault zone strikes about N45°E and is at least 50 m to as much as 400 m wide. Abbott and Goodwin (1995) noted that the fault zone in the large arroyo south of Adobe Camp is more than 160 m wide. Based on our reconnaissance mapping at Adobe Camp, the Tijeras fault has two late Quaternary strands with geomorphic expression (Fig. 2), although the fault zone may contain several strands with minor amounts of late Quaternary movement. The western strand is associated with northwest-facing topographic scarps and truncates surfaces Qp2 and Qp3. In the arroyo that traverses the site (between trenches T1A and T3, Fig. 2), an exposure of this fault strand shows Quaternary alluvium in fault contact with felsite bedrock.

The eastern strand of the Tijeras fault, located about 50 m east of the western strand, is associated with aligned saddles developed on middle to late Quaternary surfaces. The unnamed arroyo between trenches T1A and T3 has a left-lateral deflection of about 30 m across the eastern fault strand, which may be related to fault displacement. About 300 to 500 m northeast of the site, the eastern strand has excellent geomorphic expression where it crosses the Qp1 surface. Here, a 3-m-high, southeast-facing (uphill) topographic scarp may have vertical separation of 5–8 m where the Qp1 surface lies across this strand. In our opinion, the lateral variability in the amounts and senses of vertical separation along both the western and eastern primary strands suggests a large component of lateral movement along the southern Tijeras fault at Adobe Camp.

Shallow subsurface stratigraphy

Our approach to characterizing the southern part of the Tijeras fault at Adobe Camp was to expose faulted and unfaulted near-surface materials to assess the number of surface-rupture earthquakes, and to evaluate the timing of these earthquakes by estimating the ages of the associated tectonic deposits. Four exposures of the western fault strand at the Adobe Camp site were documented: (1) the 2.5-m-high southern bank of a northeast-trending unnamed gully; (2) trench T1A, which was excavated across a topographic scarp at the truncated end of surface Qp3; (3) trench T1B, which was located 1 m south of trench T1A; and (4) trench T3, which was excavated west of the truncated end of surface Qp2. In addition, the eastern fault strand was exposed in trench T2, which was excavated across a low saddle about 30 m east of trench T1A (Fig. 2). Also, four exploratory soil pits were excavated into selected piedmont surfaces (Fig. 2).

In general, the trenches and arroyo banks exposed interfingered alluvial deposits and scarp-derived colluvium northwest of the western fault strand, and fractured and sheared bedrock southeast of the western fault strand. Three highly fractured and sheared bedrock units were exposed in the trenches: Proterozoic(?) granitic rock, Triassic(?) claystone, and a light-colored Oligocene(?) porphyritic rock ("felsite"). Surficial deposits exposed in the trenches include Pleistocene and Holocene alluvial and colluvial deposits (Fig. 3). Maps of trenches

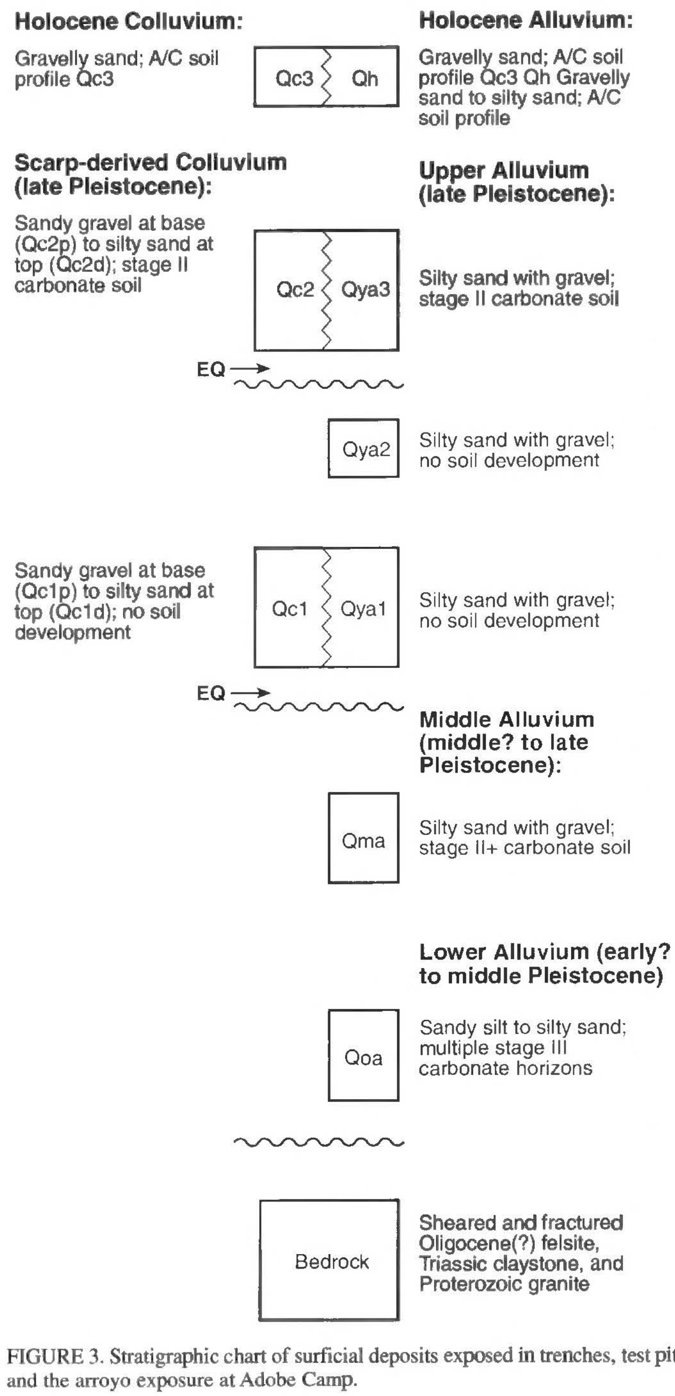

FIGURE 3. Stratigraphic chart of surficial deposits exposed in trenches, test pits and the arroyo exposure at Adobe Camp.

T1A, T1B, and T2 are shown on Figures 4, 5, and 6, respectively; the map of trench T3 is given in Kelson et al. (1998). General characteristics of the surficial geologic units are given below.

Pleistocene alluvium

Pleistocene alluvium at Adobe Camp is subdivided into the lower, middle, and upper alluviums (Fig. 3). Each of these alluvial packages contains bedded silty sand and sandy silt with minor amounts of gravel (<5–30%). In general, individual strata are upward fining and characterized by erosional basal contacts. These strata contain subangular quartzite and granitic clasts, but few or no felsite clasts. We interpret these units as alluvial deposits, rather than colluvium, because they are characterized by abrupt basal erosional contacts, subhorizontal stratification, and an absence of clasts derived from the felsite rocks that comprise the local fault scarp. The lower alluvium (unit Qoa) contains well-developed pedogenic accumulations of calcium carbonate (stage III), which suggests substantial periods of surface stability and soil formation following deposition of the alluvium. Strata within the lower alluvium are cemented with multiple discontinuous accumulations of calcium carbonate that appear to be related to vadose-zone groundwater processes, because they are not associated with other soil horizons typically produced by pedogenic processes. The abundance of groundwater-related calcium carbonate cement and multiple pedogenic soils within the lower alluvium suggests that this package may be several hundred thousand years old or perhaps older. The lower alluvium is at least 12 m thick (and probably much more) based on exposure of this unit beneath Qp2 piedmont gravel in soil pit SP3 (Fig. 2). In the trench T1A and arroyo exposures, lower alluvium is in fault contact with felsite bedrock along the western fault strand (Fig. 3).

The middle alluvium (unit Qma, Fig. 3) unconformably overlies the lower alluvium, and consists of sandy gravel and gravelly sand that fines upward into a sandy silt. The lower, coarser part of the unit contains abundant, discontinuous and subhorizontal accumulations of calcium carbonate that appear to be related to vadose-zone groundwater processes. Pedogenic calcium carbonate development (stage II+) is present in the upper part of this unit. In the trench T3 and arroyo exposures, middle alluvium is faulted and folded by the western fault strand (Kelson et al., 1998).

The upper alluvium (unit Qya) consists of sandy gravel, gravelly sand, and silty sand (Fig. 4), and is inset into middle and lower alluviums (Fig. 3). The uppermost unit within the upper alluvium (unit Qya3) contains stage II pedogenic calcium carbonate accumulations. There is no direct evidence of displacement of the upper alluvium along the western fault strand because it does not extend to the fault (Fig. 4). However, interfingering relations with the faulted colluvium (unit Qc1, described below) in trench T1A suggest that lower units (Qya1 and Qya2) within the upper alluvium pre-date at least one surface rupture earthquake at Adobe Camp. The eastern fault strand in trench T2 (Fig. 6) does not displace the uppermost unit within the upper alluvium (unit Qya3).

Scarp-derived colluvium

Immediately after a surficial faulting event, degradational processes cause deposition of colluvium adjacent to the fault scarp. This scarp-derived colluvium is direct evidence of paleoearthquakes (Nelson, 1992; McCalpin, 1996). The arroyo exposure and trenches T1A and T1B show the presence of three distinct scarp-derived colluvial units at Adobe Camp (Figs. 4 and 5). These colluvial gravels and gravelly sands characteristically contain clasts of felsite and rare or no clasts of quartzite, granitic rocks, or limestone. The colluvial deposits also are characterized by crude internal stratification that dips 7–30° to the northwest, away from the fault scarp, and proximal and distal facies

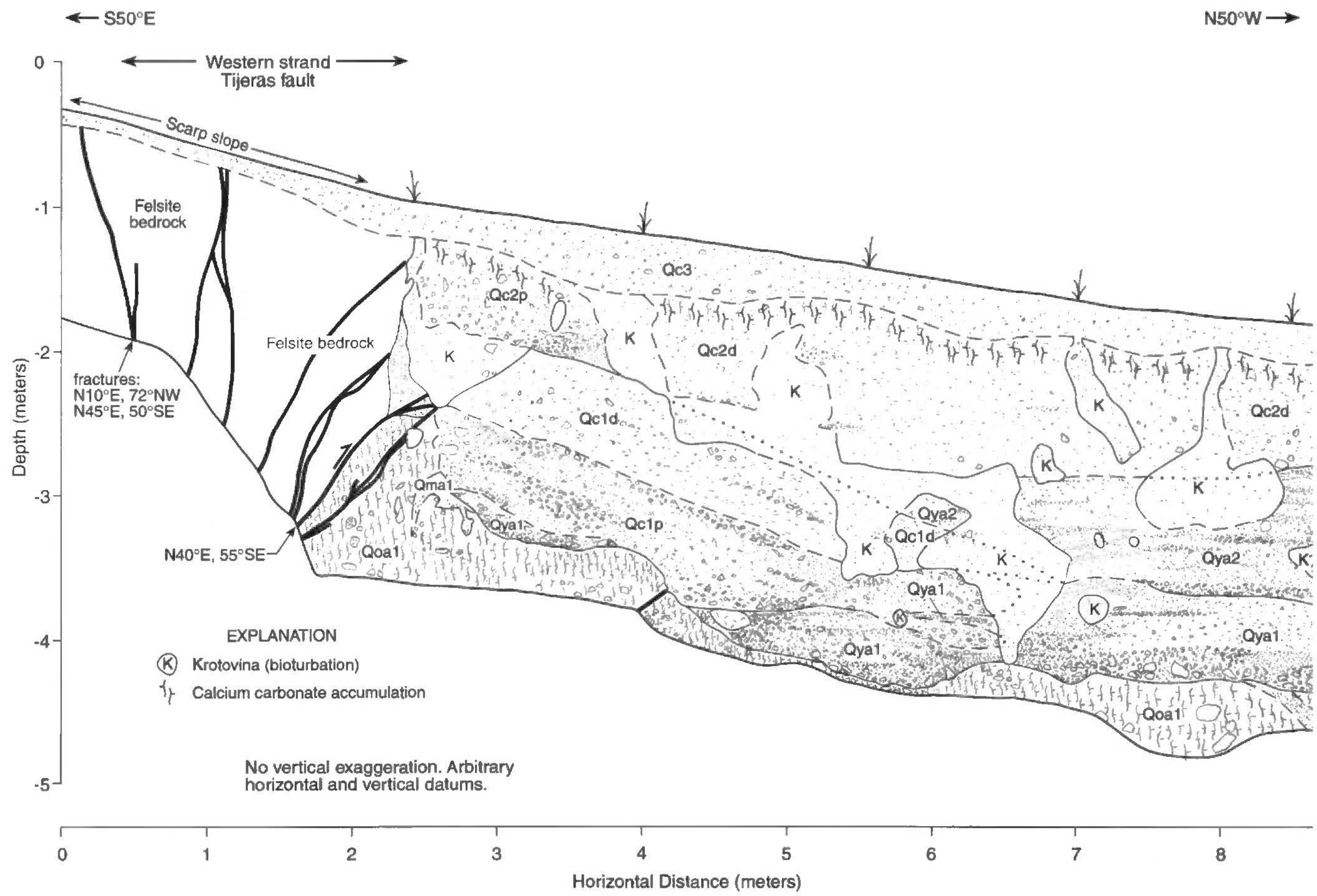

FIGURE 4. Map of southern wall of trench T1A at Adobe Camp. View toward southwest, showing western strand of the Tijeras fault.

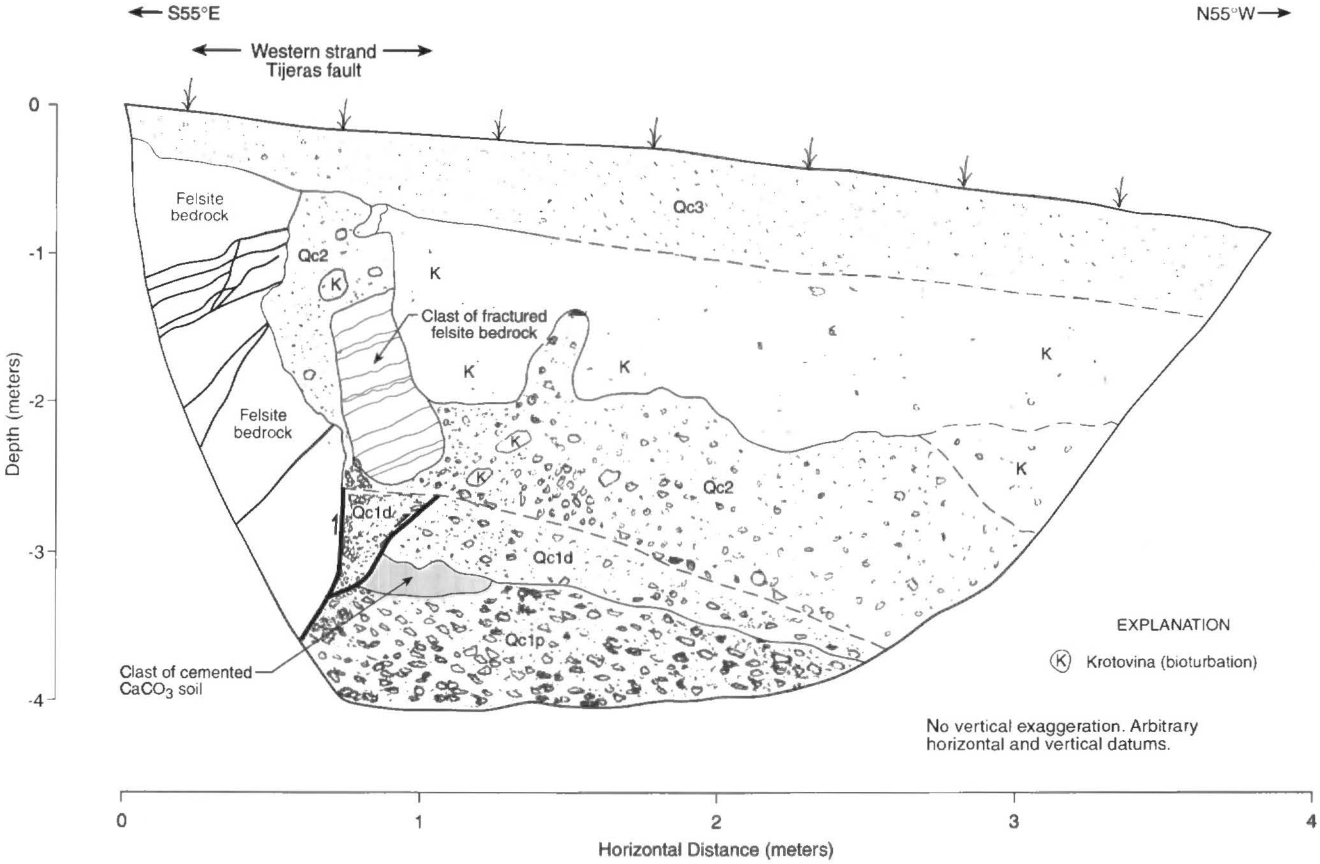

FIGURE 5. Map of southern wall of trench T1B at Adobe Camp. View toward southwest, showing western strand of the Tijeras fault. Trench T1B is located 1 m southwest of trench T1A.

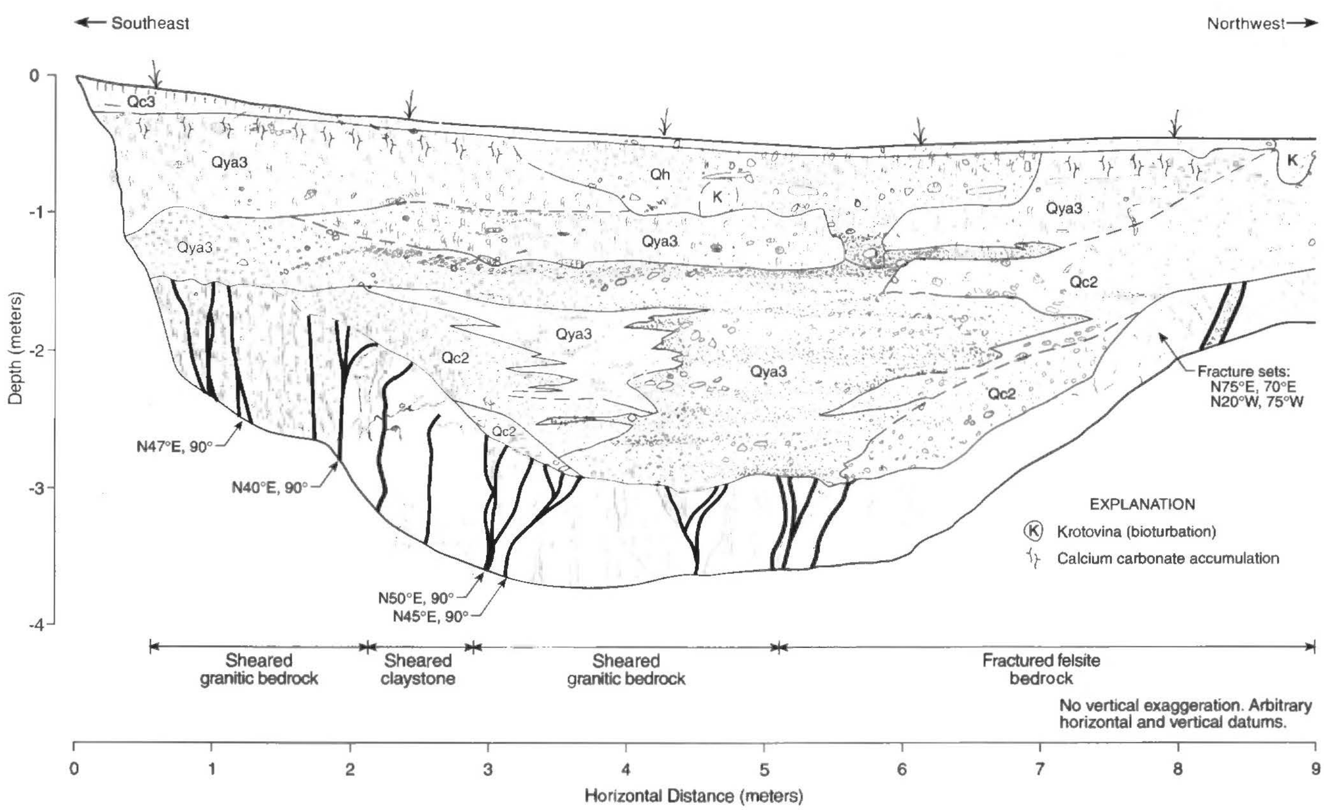

FIGURE 6. Map of southern wall of trench T2 at Adobe Camp. View toward southwest, showing eastern strand of the Tijeras fault.

indicating local derivation. The angular felsite clasts and the dip of the units distinguish them as colluvial deposits rather than alluvial deposits, which at this site contain mostly clasts of granitic rocks and quartzite derived from the drainage headwaters upstream of the fault. Colluvial units Qc1, Qc2, and Qc3 are distinguished on the basis of stratigraphic position, abrupt basal contacts, erosional unconformities, and/or fining-upward grain size.

Unit Qc1, the oldest colluvial unit, is composed of a proximal, coarse facies (subunit Qc1p, sandy gravel) and a distal fine facies (subunit Qc1d, gravelly sand). The lower proximal facies contains abundant angular and subangular clasts of felsite as much as 7 cm in diameter. In trench T1B, subunit Qc1p contains a clast of calcium-carbonate cemented silt that is about 30 cm in diameter (Fig. 5), which likely was derived from erosion of pedogenically cemented alluvium associated with the Qp3 piedmont surface. In the arroyo exposure, the subunit Qc1p stratification dips moderately to the northwest. There is no significant soil development in either subunit Qc1d or Qc1p. The northwestern part of subunit Qc1p interfingers with unit Qya1 in trench T1A (Fig. 4), and grades into the upper alluvium in the arroyo exposure. Subunit Qc1p grades upward into subunit Qc1d, which also has stratification that dips moderately northwest (Figs. 4 and 5). These relations suggest that subunits Qc1p and Qc1d were derived from a single-event fault scarp produced along the western fault strand. Notably, trenches T1A and T1B show that both subunits Qc1p and Qc1d are displaced by the western fault strand (Fig. 4 and 5).

The middle colluvial deposit (unit Qc2) also is composed of a proximal, coarse facies (subunit Qc2p, sandy gravel) adjacent to the fault and a distal fine facies (subunit Qc2d, gravelly sand to silty sand) farther from the fault (Figs. 4 and 5). The predominantly felsite clasts in subunit Qc2p are as much as 4 cm in diameter, with the exception of a large, 60 x 30 cm block in the eastern part of trench T1B (Fig. 5). This large clast is composed of fractured, sheared felsite bedrock, and is adjacent to in-place sheared felsite bedrock along the fault. The fractured nature of this block within unit Qc2p and its location adjacent to the fault strongly suggests that it likely was derived by rockfall from a bedrock scarp. Northwest of this clast, subunit Qc2p fines from sandy gravel to gravelly sand and silty sand, and essentially grades into subunit Qc2d (Fig. 5). Where not destroyed by bioturbation (see areas marked K, Figs. 4, 5), the soil in unit Qc2 is moderately developed and contains a stage II+ calcium carbonate horizon. Unit Qc2 clearly is not faulted in trench T1B, instead being in depositional contact with fractured bedrock (Fig. 5). The eastern fault strand exposed in trench T2 also does not displace colluvial unit Qc2 (Fig. 6).

Holocene alluvium and colluvium

Holocene alluvium is present on the western side of the western fault strand, and is associated with the Qh surface (Fig. 2). This alluvium is gravelly sand to silty sand, and contains clasts of quartzite and granitic rocks, as well as some reworked clasts cemented with calcium carbonate (unit Qh, Fig. 3). The deposits have soils characterized by moderate A horizon development and show evidence of stage I or less calcium carbonate accumulation. The Holocene alluvial deposits interfinger to the east with active colluvium (unit Qc3) associated with the present-day hillslopes at the site (Figs. 4–6). Neither unit Qh nor unit Qc3 is displaced by the western or eastern fault strands (Figs. 4–6).

Age estimates of surficial deposits

The ages of surficial deposits at the Adobe Camp site are poorly constrained. We estimate the ages of deposits on the basis of one radiocarbon date and the relative degree of soil development exposed in the trenches and soil pits. One charcoal fragment was analyzed from the base of unit Qh in trench T1A, which overlies unit Qc2 (Fig. 4). This sample yielded a conventional ^{14}C age of 7960 ± 40 years BP (Beta-110912, analyzed by Beta Analytic Inc., Miami), and a tree-ring calibrated age of 8770 ± 210 cal. years BP. Based on this single date, we cautiously interpret a maximum age of 8.8 ± 0.2 ka for the lower part of unit Qh. This single age estimate provides a minimum age (>8.8 ka) for unit Qya3, which is stratigraphically beneath unit Qh.

In an attempt to further estimate the ages of surficial deposits, we described and analyzed soil profiles in the four trenches and four soil pits (Fig. 2). The use of soils to constrain age estimates of those surfaces has proved to be difficult in this study. All of the soils contain calcic horizons, and a basic premise for correlating surfaces on the basis of calcic horizon development is that the degree of development of the horizon and the amount of carbonate in the soil increase with time. The main assumption is that the sources of carbonate are rainwater and particulate dust. However, alluvial deposits at the site contain some limestone clasts, which represent a source of calcium carbonate that is difficult to quantify. In addition, there is abundant evidence of ground water carbonate deposition in most of the sediments, as indicated by thick carbonate accumulations in sediments that lack other pedogenic horizons. Because this carbonate is not solely from rainwater and eolian dust, the amount of calcium carbonate in the soils provides only an estimate of the maximum age of a deposit. However, using the mass of calcium carbonate in the soil profiles and a carbonate flux derived for the Albuquerque area (Machette, 1985), we calculate that none of the soils described here is older than 100 ka. This does not agree well with other evidence for the age of landscapes in this area. Possible explanations for the apparently low calcium carbonate accumulations are that Adobe Camp is near the pedocal/pedalfer boundary, and/or that the soil profiles have been partially eroded. For example, wetter Pleistocene climates may have allowed large amounts of calcium carbonate to be flushed through the soils, and thus the soils may contain carbonate accumulated only during drier Holocene conditions. As a result, we unfortunately cannot use the profile mass of calcium carbonate to give even a maximum estimate of surface age.

Nevertheless, on the basis of stratigraphic position, the single radiocarbon date, and the moderately developed carbonate horizon in unit Qc2, we cautiously interpret a latest Pleistocene (11–30 ka) age for unit Qc2. On the basis of stratigraphic position below unit Qc2, and an absence of soil development in unit Qc1, we interpret units Qc1, Qya1, and Qya2 as late Pleistocene (30–130 ka). Furthermore, the stratigraphic position and highly oxidized nature of the middle alluvium suggest that this deposit is middle to late Pleistocene (130–750 ka). The lower alluvium is interpreted as a correlative of the Pliocene –Pleistocene Tuerto Gravel (Stearns, 1953), based on similarity to an outcrop of Tuerto Gravel that was identified by J. Hawley (personal commun., 1997) (Fig. 2). However, we acknowledge that the age estimates for all of the deposits are speculative.

Shallow subsurface structure

All four exposures across the western fault strand at Adobe Camp showed a reverse fault that strikes between about N40°E and N66°E and dips moderately (50–60°) southeast. In trenches T1A and T1B, the fault has placed highly fractured felsite bedrock against Pleistocene colluvium (Figs. 4–5). In trench T1B, the lower colluvium (unit Qc1) also is faulted against bedrock, whereas the scarp-derived colluvial unit Qc2 shows no evidence of faulting or shearing (Fig. 5). In the arroyo exposure, the lower (Qoa) and middle (Qma) alluviums are folded into a footwall syncline along the southeast-dipping fault, consistent with the west-vergent reverse displacement. In trench T3, the lower alluvium is cataclastically deformed adjacent to the southeast-dipping reverse fault, and the middle alluvium is faulted against felsite (Kelson et al., 1998). Clearly, each exposure across the western fault strand shows that reverse faulting and folding occurred in the middle to late Pleistocene.

The geometry and geomorphic expression of the eastern fault strand contrasts greatly with that of the western fault strand. Trench T2 extended across a low saddle along the eastern strand that is directly southwest of an apparent left-lateral deflection of the unnamed arroyo at the site. The trench exposed a 5-m-wide zone of vertical faults within granitic, claystone, and felsite bedrock (Fig. 6). Fractured felsite was encountered on the western side of the trench, and sheared claystone and granitic material were encountered in the central and eastern parts of the trench. The faults are vertical and strike about N45°E to N50°E.

The amount of late Quaternary vertical separation appears to differ between the eastern and western fault strands. In trench T2, near-surface bedrock is present on both sides of the eastern fault strand. Thus, the eastern strand has not had substantial vertical separation during the late Quaternary. In contrast, the absence of bedrock west of the western strand in the arroyo exposure, and in trenches T1A, T1B and T3, shows that there is substantial vertical separation across the western fault strand. The small amount of vertical separation on the eastern strand, coupled with the vertical dip, linear fault trace, geomorphic saddle, and possible left-deflection of the adjacent arroyo, suggest a substantial component of left-lateral offset along the eastern fault strand.

NUMBER AND TIMING OF QUATERNARY PALEOEARTHQUAKES

The two distinct scarp-derived colluvial units at Adobe Camp are evidence of two surface-rupture earthquakes along the Tijeras fault. We interpret that the lower colluvium represents the penultimate surface rupture, and that the faulting of the lower colluvium was produced by the most-recent rupture. The timing of these earthquakes is poorly constrained because there are considerable uncertainties in the ages of the faulted and unfaulted deposits. However, based on relative soil development and stratigraphic position, we estimate that the paleoearthquakes interpreted from the trench and arroyo exposures at Adobe Camp most likely occurred in the late Pleistocene.

We interpret that colluvial units Qc1 and Qc2 represent degradation of fault scarps produced during surface-rupturing earthquakes, for several reasons. First, the clasts within the colluvial deposits are primarily felsite, which is exposed locally only in the 30-m-wide zone between the eastern and western fault strands. In contrast, the alluvial deposits at the site contain clasts composed of granitic rock types, quartzite, or limestone, and were derived from the drainage areas southeast of the fault zone. Second, the grain-size character of the colluvial deposits suggests a genetic relation to a local fault scarp. For example, unit Qc2p in trench T1B contains a large block of fractured felsite bedrock directly adjacent to the fault. The fractured nature, angular shape, and large size of this clast, and its location adjacent to the fault, strongly suggest that it was transported a short distance and likely was derived by spalling from the bedrock scarp face. Third, the percentage and size of clasts in the colluvial deposits progressively decreases away from the fault. Both units Qc1 and Qc2 include a coarse, proximal facies near the fault and a distal facies that fines upward and away from the fault. We believe that these sedimentologic relations provide evidence that units Qc1 and Qc2 are each genetically related to scarp-producing events along the western strand of the Tijeras fault.

We interpret that the lower colluvium (unit Qc1) formed as a result of northeast-vergent reverse faulting and scarp formation along the western fault strand. Deposition of the proximal part of the lower coarse colluvium (subunit Qc1p) likely occurred closely following formation of the scarp. The stratigraphic position of unit Qc1 suggests that this rupture occurred after deposition of the lower and middle alluviums, which are strongly deformed along the fault. The interfingering relationship between unit Qc1 and alluvium Qya1 (Fig. 3) suggests that this rupture occurred during the deposition of alluvium Qya1. Although the ages of these units are unknown, we interpret units Qc1, Qya1, and Qya2 as late Pleistocene, and therefore, this penultimate rupture may have occurred during the late Pleistocene.

We also interpret a second, more recent rupture along the western fault strand, on the basis of: (1) faulting of the lower colluvium, and (2) the presence of unfaulted scarp-derived colluvial unit Qc2 overlying the faulted lower colluvium. In trenches T1A and T1B, the lower colluvium (unit Qc1) clearly is faulted (Figs. 4 and 5), suggesting a surface rupture following the deposition of this unit. Notably, in trench T1B, the shear planes that cut unit Qc1 do not extend into the overlying colluvial unit Qc2 (Fig. 5). This same trench exposes the large block of fractured bedrock within the proximal facies of unit Qc2, which is suggestive of spalling from a fresh scarp face. Thus, we interpret that the proximal facies of unit Qc2 (subunit Qc2p) was deposited closely following the most recent surface rupture. The age of unit Qc2 is poorly constrained, but likely is older than about 8.8 ka, the age of the lower part of the overlying Holocene alluvium. The moderate soil developed in unit Qc2 (stage II calcium carbonate morphology) supports an age of at least several thousand years. As noted above, we cautiously interpret a latest Pleistocene age for unit Qc2. If our interpretation that the penultimate rupture occurred during the late Pleistocene is correct, then it appears that there have been at least two surface ruptures on the southern Tijeras fault since the middle Pleistocene (<130 ka).

LOCAL STRUCTURAL MODEL

The two fault strands at Adobe Camp have distinct differences in geometry and probable sense of separation. The western fault strand exhibits northwest-vergent reverse faulting along southeast-dipping planes, and the eastern strand is characterized by faulting along vertical planes that separate slivers of several bedrock types, with little or no late Quaternary vertical separation. Based on field mapping, the arroyo exposure, and trenches T1 and T2, the western fault strand appears to be a moderately dipping reverse fault that probably merges with the vertical eastern fault strand at a depth of about 30 to 40 m (Fig. 7). The eastern fault strand probably is dominated by left-lateral slip, based on its vertical dip, lack of substantial vertical separation, linear fault trace, and possible left-deflection of the unnamed arroyo. These data support previous interpretations of left-lateral slip on the Tijeras fault (Abbott and Goodwin, 1995), as well as our interpretation that the Tijeras fault at Adobe Camp is a positive half-flower structure. During surface-rupture earthquakes on the southern part of the Tijeras fault, a large component of the vertical separation appears to be accommodated along the western strand, and left-lateral offset probably is accommodated primarily on the eastern strand. The late Quaternary kinematics along the southern Tijeras fault, therefore, support the interpretation that "strain partitioning" (Lettis and Hanson, 1991) has occurred at a shallow depth at Adobe Camp.

APPLICATION TO SEISMIC HAZARD ASSESSMENT

This investigation provides information that allows a better characterization of the Tijeras-Cañoncito fault system for seismic hazard

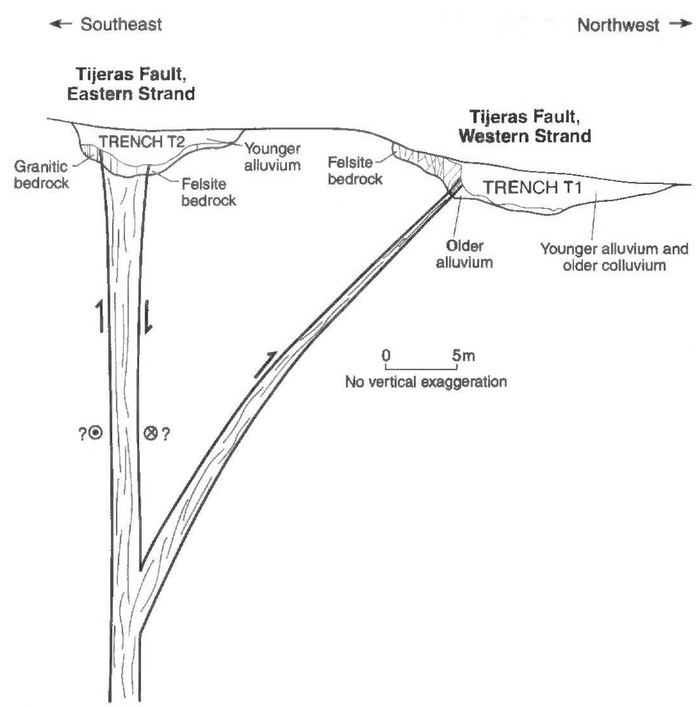

FIGURE 7. Schematic diagram showing generalized stratigraphic and structural relations exposed in trenches T1A and T2 at Adobe Camp, and hypothesized down-dip merge of the western and eastern fault strands. Strain partitioning suggested by reverse separation on the western fault strand and possible lateral offset along the eastern fault strand.

assessments. Because of the paucity of paleoseismic data on the Tijeras-Cañoncito fault system, there are considerable uncertainties in the location, length, and activity of potential fault rupture sections. The Tijeras-Cañoncito fault system consists of at least two primary physical sections: the 41-km-long Canyon section between Albuquerque and the village of Golden, and the 51-km-long Galisteo section between Golden and the village of Cañoncito (Machette et al., 1998). This study provides evidence of two late Quaternary surface ruptures along the Canyon section of the fault. Previous studies showing evidence for late Quaternary displacement near Albuquerque (GRAM/William Lettis & Associates, 1995), in Tijeras Canyon (Lisenbee et al., 1979), and near Golden (Abbott and Goodwin, 1995), therefore suggest that the entire Canyon section of the fault could rupture during a single earthquake. Based on empirical relations between fault length and earthquake magnitude (Wells and Coppersmith, 1994), a rupture of the entire 41-km-long Canyon section may produce an earthquake of about $M_W 7.0$, considerably larger than any earthquake felt historically in central or northern New Mexico.

SUMMARY AND CONCLUSIONS

The 100-km-long Tijeras-Cañoncito fault system is a potential seismogenic source that extends between the Santa Fe and Albuquerque metropolitan areas of New Mexico. The fault system accommodates east-west crustal extension and provides structural linkage between the Española and Albuquerque basins of the active Rio Grande rift. At the Adobe Camp site northeast of Albuquerque, we conducted trenching to assess the near-surface location, timing, and style of late Quaternary deformation on the southern Tijeras fault, a major component of the Tijeras-Cañoncito fault system. At Adobe Camp, the fault consists of two main strands that may represent a positive half-flower structure. The eastern fault strand is vertical and coincides with a left-deflection in a west-flowing arroyo. The western fault strand has reverse fault geometry and dips moderately eastward; it likely merges with the eastern vertical strand in the shallow subsurface (about 30 to 40 m depth). The western strand has placed bedrock over late Quaternary deposits and coincides with northwest-facing scarps that truncate piedmont surfaces. We interpret that during surface-rupturing earthquakes on the southern Tijeras fault at Adobe Camp, vertical separation was produced along the western fault strand, and lateral offset occurred primarily on the eastern fault strand. Trench and arroyo-wall exposures show that two colluvial deposits were shed from the fault scarps along the western fault strand. The lower colluvial deposit is faulted, whereas the upper colluvium is not, thereby indicating two faulting events. Our interpretation is that the scarp-derived colluvia were deposited following two surface-rupturing earthquakes. The ages of these earthquakes are poorly constrained because of uncertainties in the ages of the faulted and unfaulted colluvia. However, based on the relative degree of soil development and stratigraphic position, we estimate that the colluvia most likely are late Pleistocene (11–130 ka), and interpret the occurrence of two surface ruptures along the southern Tijeras fault during the late Pleistocene (<130 ka). If these earthquakes ruptured the entire 41-km-long southern part of the Tijeras fault, they may have been as large as M_W 7.0.

ACKNOWLEDGMENTS

We thank Ron Pisk of the Campbell Farming Corporation for permission to conduct the investigations at Adobe Camp. We also thank Frank Pazzaglia (University of New Mexico) for showing us the arroyo exposure at Adobe Camp. Missy Eppes (New Mexico Tech) helped log trenches, and Harland Goldstein (New Mexico Tech) helped map the geomorphic surfaces at the site and describe soil pits. Laurel Goodwin, Sean Connell, Mike Skelly and many others provided useful comments during a field review of the trenching. This research was supported by the U.S. Geological Survey (USGS, Department of the Interior), under USGS award number 1434-HQ-97-GR-03012. The views and conclusions contained in this document are those of the authors and should not be interpreted as necessarily representing the official policies, either expressed or implied, of the U.S. Government.

REFERENCES

Abbott, J. C. and Goodwin, L. B., 1995, A spectacular exposure of the Tijeras fault, with evidence for Quaternary motion: New Mexico Geological Society, Guidebook 46, p. 117–125.

Ferguson, C., Timmons, M., Pazzaglia, F., Karlstrom, K. and Bauer, P., 1996, Geology of the Sandia Park 7.5-minute quadrangle, Bernalillo and Sandoval Counties, New Mexico: New Mexico Bureau of Mines and Mineral Resources, Open-file Digital Geologic Map OF-DGM 1, scale 1:12,000.

GRAM, Inc. and William Lettis & Associates, Inc., 1995, Conceptual geological model of the Sandia National Laboratories and Kirtland Air Force Base: Technical Report submitted to the Site-wide Hydrogeologic Characterization Project, Organization 7584, Environmental Restoration Program, Sandia National Laboratories, Albuquerque, New Mexico, 2 volumes, various pagination, 5 appendices.

Karlstrom, K. E., Connell, S. D., Ferguson, C. A., Read, A. S., Osburn, G. R., Kirby, E., Abbott, J., Hitchcock, C., Kelson, K., Noller, J., Sawyer, T., Ralser, S., Love, D. W., Nyman, M. and Bauer, P. W., 1994, Geology of the Tijeras 7.5-minute quadrangle, Bernallilo County, New Mexico: New Mexico Bureau of Mines and Mineral Resources, Open-file Digital Geologic Map OF-DGM 4, scale 1:12,000.

Kelley, V. C. and Northrop, S. A., 1975, Geology of Sandia Mountains and vicinity, New Mexico: New Mexico Bureau of Mines and Mineral Resources, Memoir 29, 136 p.

Kelson, K. I., Hitchcock, C. S., Sawyer, T. L., Thomas, E. C. and Gibson, J. D., 1994, Reducing uncertainty in assessment of the hydrogeologic framework—Characterization of surficial deposits at Sandia National Laboratory, New Mexico (abs.): EOS Transactions of the American Geophysical Union, Supplement, v. 75, no. 44, p. 278.

Kelson, K. I., Hemphill-Haley, M. A., Olig, S. S., Simpson, G. D., Gardner, J. N., Reneau, S. L., Kolbe, T. R., Forman, S. L. and Wong, I. G., 1996, Late Pleistocene and possibly Holocene displacement along the Rendija Canyon fault, Los Alamos County, New Mexico: New Mexico Geological Society, Guidebook 47, p. 153–160.

Kelson, K. I., Hitchcock, C. S. and Harrison, J. B. J., 1998, Paleoseismologic assessment of the southern Tijeras fault, central New Mexico: Final Technical Report submitted to the U.S. Geological Survey, Contract No. 1434-HQ-97-GR-03012, National Earthquake Hazards Reduction Program, 33 p.

Lettis, W. R. and Hanson, K. L., 1991, Crustal strain partitioning: implications for seismic hazard assessment in western California: Geology, v. 19, p. 559–562.

Lisenbee, A. L., Woodward, L. A. and Connolly, J. R., 1979, Tijeras-Cañoncito fault system—A major zone of recurrent movement in north-central New Mexico: New Mexico Geological Society, Guidebook 30, p. 89–99.

Machette, M. N., 1978, Dating Quaternary faults in the southwestern United States by using buried calcic paleosols: U.S. Geological Survey, Journal of Research, v. 6, p. 369–382.

Machette, M. N. and McGimsey, R. G., 1983, Quaternary and Pliocene faults in the Socorro and western part of the Fort Sumner 1° x 2° quadrangles, central New Mexico: U.S. Geological Survey, Miscellaneous Field Studies Map MF-1465-A, with pamphlet, scale 1:250,000.

Machette, M. N. and Personius, S. F., 1984, Quaternary and Pliocene faults in the eastern part of the Aztec quadrangle and the western part of the Raton quadrangle, Northern New Mexico: U.S. Geological Survey, Map MF-1465-B, with pamphlet, scale 1:250,000.

Machette, M. N., Personius, S. F., Kelson, K. I., Dart, R. L. and Haller, K. M., 1998, Map and data for Quaternary faults in New Mexico: U.S. Geological Survey, Open-file Report 98-521, 1 plate, 1:750,000 scale.

McCalpin, J. M., 1996, Paleoseismology in extensional tectonic environments; *in* McCalpin, J. M., ed., Paleoseismology: Academic Press, San Diego, p. 85–146.

Nelson, A. R., 1992, Lithofacies analysis of colluvial sediments—an aid in interpreting the recent history of Quaternary normal faults in the Basin and Range Province, western United States: Journal of Sedimentary Petrology, v. 62, p. 607–621.

Olsen, K. H., 1979, The seismicity of north-central New Mexico with particular reference to the Cerrillos earthquake of May 28, 1918: New Mexico Geological Society, Guidebook 30, p. 65–75.

Sanford, A. R., Jaksha, L. H. and Cash, D. J., 1991, Seismicity of the Rio Grande rift in New Mexico; *in* Slemmons, D. B., Engdahl, E. R., Zoback, M. D. and Blackwell, D. D., eds., Neotectonics of North America: Geological Society of America, Decade Map 1, p. 229–244.

Smith, L. N., Bullard, T. F. and Wells, S. G., 1982, Quaternary geology and geomorphology of Tijeras Canyon, New Mexico: New Mexico Geological

Society, Guidebook 33, p. 5–8.
Sandia National Laboratories (SNL), 1995, Site-Wide Hydrogeologic Characterization Project, Calendar Year 1994 Annual Report—Environmental Restoration Project: U.S. Department of Energy, Albuquerque Operations Office, 4 sections, various pagination, 14 appendices.
Stearns, C. E., 1953, Tertiary geology of the Galisteo-Tonque area, New Mexico: Geological Society of America Bulletin, v. 64, p. 459–508.
Wells, D. L. and Coppersmith, K. J., 1994, New empirical relationships among magnitude, rupture length, rupture width, rupture area, and surface displacement: Seismological Society of America Bulletin, v. 84, p. 974–1002.
Wong, I. and 16 others, 1995, Seismic hazards evaluation of the Los Alamos National Laboratory: Oakland, California: Woodward Clyde Federal Services, Final Report for Los Alamos National Laboratory, Los Alamos, New Mexico, 2 volumes, various pagination, 16 appendices.
Wong, I., Kelson, K., Olig, S., Bott, J., Green, R., Kolbe, T., Hemphill-Haley, M., Gardner, J., Reneau, S. and Silva, W., 1996, Earthquake potential and ground shaking hazard at the Los Alamos National Laboratory, New Mexico: New Mexico Geological Society, Guidebook 47, p. 135–142.

Charlie Read, Gordon Wood, and Bob Murphy wait for the discussion to begin at a roadstop on the second day of the 1st field conference in 1950 (photograph courtesy of Florence Wengerd).